

Systems analysis of a quorum sensing network: Design constraints imposed by the functional requirements, network topology and kinetic constants

A.B. Goryachev*, D.J. Toh, T. Lee

Systems Biology Group, Bioinformatics Institute, 30 Biopolis Str., Singapore 138671, Singapore

Received 12 January 2005; received in revised form 11 April 2005; accepted 14 April 2005

Abstract

Understanding the relationship between the structural organization of intracellular decision networks and the observable phenotypes they control is one of the exigent problems of modern systems biology. Here we perform a systems analysis of a prototypic quorum sensing network whose operation allows bacterial populations to activate certain patterns of gene expression cooperatively. We apply structural perturbations to the model and analyze the resulting changes in the network behavior with the aim to identify the contribution of individual network elements to the functional fitness of the whole network. Specifically, we demonstrate the importance of the dimerization of the transcription factor and the presence of the auxiliary positive feedback loop on the switch-like behavior of the network and the stability of its “on” and “off” states under the influence of molecular noise.

© 2005 Elsevier Ireland Ltd. All rights reserved.

Keywords: Quorum sensing; Gene expression network; Systems biology; Mathematical modeling

1. Introduction

Complex behavior of biological systems is a phenotypical manifestation of the operation of intracellular circuitry composed of signal transduction and gene expression networks. The promise of systems biology to understand how molecular networks control the observed behavior relies on the hope that the entire decision circuitry can be hierarchically decomposed into functional modules of progressively lower complexity (Hartwell et al., 1999). The first step along this path is to identify the most fundamental control modules (Milo et al., 2002) and fully understand their function. One strategy to achieve this goal is to apply a multitude of perturbations to the network components and observe

the changes in system behavior (Ideker et al., 2001). This task is not trivial because the function of a network is not just a linear combination of the functions of its parts. Additional complexity arises from the fact that most of networks perform their function on a hierarchy of systemic levels from the molecular to population-wide. The situation is not uncommon when the mechanics of a certain network is well characterized on the molecular level, but its function on higher systemic levels is barely understood.

Here we develop an *in silico* perturbation approach that can be applied to model control networks to gain insight into the significance of their components for the functional fitness of whole networks. Specifically, we investigate a prototypic network that controls the quorum sensing phenomenon. This network has emerged as a generalization of a number of individual control networks found in a broad range of Gram-negative bacterial species. Quorum sensing (QS) is a token name for

* Corresponding author. Tel.: +65 64788269.

E-mail address: andrewg@bii-sg.org (A.B. Goryachev).

the ability of bacterial populations to cooperatively activate specific gene expression programs in response to the increase in local cell density (von Bodman et al., 2003; Henke and Bassler, 2004; Fuqua and Greenberg, 2002; Fuqua et al., 2001).

The cell–cell communication that is necessary to coordinate the collective behavior is achieved through the mechanism that can be considered a biochemical analogy of radar. Each individual cell secretes a certain amount of diffusible, low-molecular-weight substance termed autoinducer, whose local concentration can be perceived by other bacteria present in the surrounding environment. In the absence of other autoinducer-producing cells and impenetrable boundaries, diffusion rapidly disperses the newly synthesized molecules of autoinducer and they are eventually lost in the environment like the probing signal of radar. Once a certain threshold density of autoinducer-producing cells is reached, the incoming autoinducer signal amplified by the QS network turns on the expression of the phenotype-specific genes and boosts the production of autoinducer. The relationship between the structural organization of such a network and its biological function is the focus of the present work.

The acyl-homoserine lactone signaling system typical to Gram-negative bacteria and considered in detail in this paper is not the only known implementation of the quorum sensing protocol. Thus Gram-positive bacteria utilize secreted peptides to achieve the same density-dependent effect (for review see Fuqua and Greenberg, 2002). Additional communication system that relies on a secreted metabolite termed AI-2 was found uniformly in both types of bacteria (see e.g., Henke and Bassler, 2004).

1.1. Functional requirements

Quorum sensing is a system of choice for the structure–function analysis because its functional requirements are thought to be well understood. The intracellular dynamics of the QS network can be readily linked to the observed bacterial population behavior both experimentally and theoretically (McMillen et al., 2002; Basu et al., 2004; You et al., 2004). All known QS networks operate as an “on–off” gene expression switch by controlling the level of a certain transcription factor whose expression is suppressed in the “off” state and is strongly induced in the “on” state. A QS network therefore is expected to possess a sharp switch-like behavior in response to variation of autoinducer in the environment. Until a certain critical autoinducer concentration is reached, the intracellular network must remain in the

“off” state with a stand-by level of autoinducer production and less than one molecule of transcription factor per cell. Above the threshold, the transcription factor is expected to be found in detectable concentrations sufficient to stably activate expression of all target operons. Typically such behavior implies a bistable, hysteretic form of the relationship between the transcription factor copy number and the extracellular concentration of autoinducer.

Provided that the typical bacterial cell volume is in the range 10^{-13} to 10^{-12} cm³, most of RNA and some protein species, especially in the “off” state, are present in the order of 10 and less copies per cell. The QS network should thus be able to exert its control and exhibit the switch-like behavior in the conditions of intensive molecular noise. Specifically, this implies that the “off” state should be robust to fluctuations in the copy number of the network components. Moreover, not only the average level of the QS transcription factor but also its fluctuations should be kept under tight control. If at a very low extracellular concentration of autoinducer the transcription factor copy number exhibited rare but large deviations from zero, a bacterial population at any time would have a certain percentage of cells in the “on” state. This is likely to be detrimental for the individuals in the “on” state and potentially for the entire population. For example, if the QS-controlled phenotype is an expression of toxins or other virulence factors, the “forerunners” would give the host organism an advanced notification of a pending attack and possibly trigger the immune response.

Additional requirements stem from the population-wide nature of the QS phenomenon. To perform the transition, the population needs to produce a supercritical concentration of autoinducer in a macroscopic volume. If the value of the critical concentration were too high, it would imply a waste of the population resources, potential detection by the host, competitors, or predators and the inability to reach QS in the conditions unfavorable for the accumulation of autoinducer (e.g., in the presence of flow). The threshold population density that is required to achieve the critical autoinducer concentration has to be within the range natural for the environment where the particular QS event takes place, e.g., in the light organ of a squid or in the rhizosphere of a plant. In most cases, bacterial population density is constrained by the availability of nutrients, presence of competitors or the host response and the QS network has to comply with the restriction on the maximum density. For example, this implies that the production of autoinducer in the “off” state should be sufficient to accumulate the critical concentration at a permissible cell density.

Some of the discussed requirements are contradicting each other and the fulfillment of their entirety is a non-trivial task that requires evolutionary optimization. For example, the necessity to produce an appreciable amount of autoinducer in the “off” state is countered by the need to maintain a low copy number of the transcription factor. Given these restrictions, one may expect that the network layouts selected by evolution are functionally optimized and all network components are important for the functional fitness. By perturbing these networks we can learn how the affected components contribute to the observed phenotype. A prototypic QS network layout has emerged from a number of studies in various Gram-negative bacterial species (Fuqua et al., 2001). Here we analyze this network paradigm by altering its layout *in silico* and estimating the resulting changes in the functional fitness of the network by means of computational modeling.

2. The model

2.1. The QS network topology

The first detailed molecular characterization of the QS phenomenon appeared in the studies of density-dependent regulation of bioluminescence in a squid symbiont *Vibrio fischeri* (Engebrecht and Silverman, 1984; Engebrecht et al., 1983). They demonstrated that the production of light is controlled by two regulatory proteins LuxR and LuxI that act as the transcription factor that activates expression of the light-producing enzyme luciferase and the autoinducer synthase, respectively. More than 20 years later we know dozens of QS network layouts in various Gram-negative bacteria that are based on the homologues of the LuxR–LuxI couple (Fuqua et al., 2001; von Bodman et al., 2003; Fuqua and Greenberg, 2002). These proteins play key roles also in our model QS network, which is shown in Fig. 1, and are denoted simply as R and I. Synthase I produces autoinducer out of readily available in the cell metabolites, which are assumed to be present in excess and are denoted as a single substrate S for brevity. The synthesized molecules of autoinducer A can freely diffuse through the cell wall equilibrating the intracellular and extracellular pools of autoinducer. Although in some bacterial systems this process has been shown or suspected to be facilitated by active transport (Fuqua et al., 2001), generally it relies on passive permeability of the cell wall (Fuqua et al., 2001; von Bodman et al., 2003; Fuqua and Greenberg, 2002). Binding of A to the monomeric R protein results in the creation of a product P that is either immediately transcriptionally competent, or after the dimerization that results in a dimeric

form D. Both binding reactions are considered here as reversible (Fuqua et al., 2001) although in some species the formed complexes are exceptionally stable (see Section 3.1 for discussion). The formed transcription factor (either P or D) directly activates transcription of the operon containing synthase I and other operons coding for the phenotype-specific genes. Activation of the transcription occurs through the specific reversible binding of the transcription factor to the response sequences located in the immediate proximity of the target operon promoters. This in turn causes recruitment of the RNA polymerase and increases the frequency of the transcription initiation (Fuqua et al., 2001). In many cases the transcription factor also activates expression of the protein R creating additional positive feedback. Assembling all of the described molecular interactions together with the processes of transcription, translation and degradation of the components, we obtain a self-contained prototypical network presented in Fig. 1. Although exactly this layout can hardly be attributed to any existing bacterial species, it can be found as a network motif in almost all Gram-negative bacteria. Real networks typically demonstrate higher complexity which is achieved through addition of supplementary positive and negative feedback loops (Zhu et al., 2000) as well as through the modular design involving parallel and sequential arrangement of individual QS modules (Wisniewski-

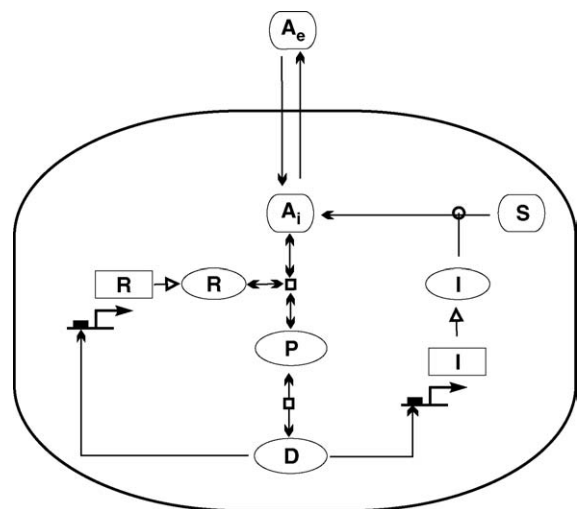
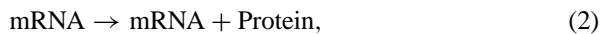
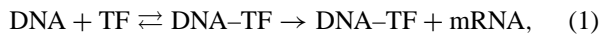


Fig. 1. A prototypic quorum sensing network layout of Gram-negative bacteria. Proteins are shown as ellipses and mRNA species as rectangles. R and I are quorum sensing transcription activator and autoinducer synthase of LuxR–LuxI type. A_i and A_e denote internal and external concentrations of autoinducer, respectively. P and D represent the complex of R and autoinducer and the dimer of this complex. S denotes substrates of the autoinducer synthase. Empty circle arrowheads represent enzymatic catalysis and empty triangles the transcription. Reversible reactions of formation of P and D are denoted as empty boxes.

Dye and Downie, 2002; Ledgham et al., 2003). In this paper we consider a QS module consisting of two positive feedback loops, the obligatory QS loop R–P(D)–I and the optional amplification loop R–P(D)–R. Specifically, we study the contribution of the transcription factor dimerization and the influence of the second feedback loop.

2.2. Modeling approach

We use a standard chemical kinetic approach based on the mass-action rate law to describe temporal dynamics of the intracellular QS network while the extracellular concentration of autoinducer, A_e , is varied as a free parameter. Complex processes of transcription and translation are considered in a simplified cumulative form:



where TF is either P or D. This approach leads to the systems of ordinary differential equations that can be studied analytically and simulated numerically. To investigate the influence of molecular noise on network components, we go beyond standard ODE formalism and simulate the network kinetic equations with the exact Gillespie algorithm (Gillespie, 1977) as implemented in the public-domain whole-cell modeling software package Cellware (Dhar et al., 2004a,b). Kinetic parameters used in our models were estimated on the basis of the published data. Assuming that a generic bacterial cell can be approximated by a cylinder with radius $0.3 \mu\text{m}$ and length $2 \mu\text{m}$, we calculated the bacterial cell volume $V_b = 5.65 \times 10^{-13} \text{cm}^3$ and cell surface area $S_b = 4.34 \times 10^{-8} \text{cm}^2$. Given that the permeability of the cell wall to autoinducer is on the order of $P \approx (1-5) \times 10^{-6} \text{cm/s}$ (Kaplan and Greenberg, 1985; Rubinow, 2002), the estimate for the autoinducer diffusivity is $k_{14} = PS_b/V_b = 0.08-0.4 \text{s}^{-1}$. Using the value of V_b , we converted all concentrations from moles per liter (M) to molecules per cell and adjusted the appropriate kinetic constants (1 molecule per cell corresponds to approximately 3 nM). These measurement units facilitate the interpretation of results and can be used interchangeably between the deterministic and stochastic modeling approaches. All deterministic simulations were performed using Matlab (The MathWorks Inc., Natick, MA).

3. Results and discussion

3.1. Stability of the transcription factor

Formation of the complex between autoinducer and the monomeric R protein provides an example of a single molecular interaction so crucial for the function of the whole network that the value of the constant describing its kinetics can invalidate the entire layout. In the recent modeling literature it has been implicitly assumed that complex P is unstable and its concentration is in quasi-equilibrium with concentrations of A and R at all times (James et al., 2000; Dockery and Keener, 2001). Slow formation of P and its fast dissociation guarantee that the level of P is negligible when the abundance of R and A are low. Recent results of Urbanowski et al. (2004) on the interaction between *V. fischeri* LuxR and its cognate autoinducer appear to back up this hypothesis. These authors found the formation of the complex easily reversible and measured the dissociation constant to be approximately 100 nM. Low stability of the complex between R and A however is not the case for all known QS networks of LuxR–LuxI type. A striking counter example is provided by the interaction of *Agrobacterium tumefaciens* TraR protein and its autoinducer AAI. Their binding is thought to occur only during TraR translation when the newly synthesized protein chain tightly wraps around the autoinducer molecule (Zhu and Winans, 1999; Zhu and Winans, 2001). Structural studies (Zhang et al., 2002) confirmed that this complex can be considered practically irreversible as the AAI molecule is buried deeply inside the protein and is not accessible to the solvent. For the network topology shown in Fig. 1, a strong bias of the binding equilibrium towards P results in the accumulation of the transcription factor that continues until the network reaches the “on” state. This process does not require the influx of the extracellular autoinducer and the “on” state is reached at any value of A_e . Thus if complex P is very stable, the network layout considered in this paper fails to provide the required behavior of an “on-off” switch. Interestingly, in the *A. tumefaciens* QS network this problem is resolved through the introduction of an additional negative feedback loop that assures the near-zero level of the transcription factor in the “off” state (Hwang et al., 1999; Swiderska et al., 2001).

The stability of the complex P can be defined more precisely on the basis of the following inequality. If the half-life of the complex P due to the process of dissociation is much shorter than its half-life due to the protein degradation $t_{1/2}^{\text{dis}} \ll t_{1/2}^{\text{deg}}$, the complex can be considered unstable and the assumption of its quasi-equilibrium

with A and R valid. If, on the contrary, $t_{1/2}^{\text{deg}} \ll t_{1/2}^{\text{dis}}$, P is stable during its lifetime and our network layout does not describe a functional QS network. Similar qualitative arguments apply if complex P undergoes dimerization but the quantitative analysis becomes much more complex. Here we restrict our consideration to the case when both binding equilibrium constants favor the dissociation of the complexes.

3.2. The minimal QS network

We first asked if a functional QS network that satisfies the formulated requirements can be designed solely on the basis of the obligatory QS loop R–P(D)–I without the supporting the amplification loop R–P(D)–R. Since such a layout has the minimal possible complexity, in the following we refer to this network as minimal. To perform qualitative analysis of the network dynamics, we reduce the dimensionality of the minimal QS network applying standard quasi-steady-state approximation. Variables describing vacant transcription factor binding sites and DNA-TF complexes (see Eq. (1)) can be readily eliminated using effective Michaelis–Menten approximation for all transcription events. We further assume that both in the “off” and “on” states the steady-state approximation can be applied to all mRNA species and the autoinducer synthase I. Keeping D in the network layout we then obtain the following kinetic equations:

$$\frac{dR}{dt} = \frac{k_1 k_6}{k_2} - k_7 R, \quad (3)$$

$$\frac{dA_i}{dt} = \frac{k_{11} k_9}{k_5 k_{10}} \left(\frac{k_3 D}{K_4 + D} + k_{12} \right) - k_8 R A_i + k_{-8} P + k_{14} (A_e - A_i), \quad (4)$$

$$\frac{dP}{dt} = k_8 R A_i - k_{-8} P - 2k_{13} P^2 + 2k_{-13} D, \quad (5)$$

$$\frac{dD}{dt} = k_{13} P^2 + k_{-13} D. \quad (6)$$

The form of Eqs. (5) and (6) incorporates the earlier stated conjecture that both P and D are unstable complexes in the sense that $t_{1/2}^{\text{dis}} \ll t_{1/2}^{\text{deg}}$. The degradation terms are therefore omitted from the equations as negligible in comparison with the dissociation terms. Applying steady-state approximation to P and D and expressing R from Eq. (3) we finally reduce the entire system to a single nonlinear equation for the concentration of autoinducer:

$$\frac{dA_i}{dt} = \frac{k_{11} k_9}{k_5 k_{10}} \left(\frac{k_3 A_i^2}{K_4 / K_{13} k_8^2 R_0^2 + A_i^2} + k_{12} \right) + k_{14} (A_e - A_i), \quad (7)$$

where $R_0 = k_1 k_6 / k_2 k_7$ is the stationary autoinducer-independent level of R. As shown in Fig. 2A, Eq. (7) can potentially describe an “on–off” switch whose dynamics is controlled by the extracellular concentration of autoinducer A_e . Interestingly, we find that the dimerization of the transcription factor is essential for this network property. This can be readily shown if the dimerization step is removed from the reaction mechanism and the kinetic equations are modified accordingly. Following the same steps, instead of (7) we find the equation:

$$\frac{dA_i}{dt} = \frac{k_{11} k_9}{k_5 k_{10}} \left(\frac{k_3 A_i}{K_4 / K_8 R_0 + A_i} + k_{12} \right) + k_{14} (A_e - A_i), \quad (8)$$

that has a single stationary state at all values of A_e and does not possess the switch-like behavior. Thus the network layout with dimerization of the transcription factor

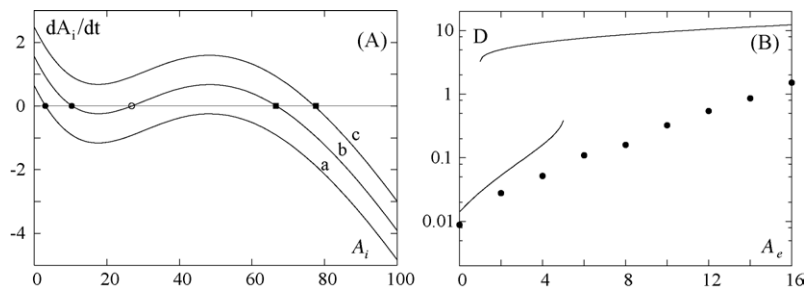


Fig. 2. Dynamics of the minimal quorum sensing network. (A) Dependence of the autoinducer production on the concentration of autoinducer according to Eq. (7) with parameters given in Table 1 plotted at three values of extracellular autoinducer concentration: (a) 0 nM; (b) 12 nM; (c) 24 nM. Positions of stable stationary states are marked by filled circles for the “off” network state and by filled boxes for the “on” state. (B) Dependence of the D concentration on A_e , deterministic bifurcation diagram is shown by lines and time-averaged value of D in the stochastic model by filled circles (observation time 6×10^6 s, sampled every 100 s). A_e concentration is shown as molecules per cell.

Table 1
Kinetic constants used in the model of the minimal QS network

Constant	Legend	Value	References
k_1	Transcription of R	$1.5 \times 10^{-2} \text{ m s}^{-1}$	Dundr et al. (2002), Kierzek et al. (2001) and Iyer and Struhl (1996)
k_2	Degradation of R mRNA	$6.0 \times 10^{-3} \text{ s}^{-1}$	Hambraeus et al. (2003)
k_3	Transcription of I, maximal velocity	$1.4 \times 10^{-2} \text{ m s}^{-1}$	Dundr et al. (2002), Kierzek et al. (2001) and Iyer and Struhl (1996)
k_4	Transcription of I, binding of D, “on” rate	$10^{-2} \text{ m}^{-1} \text{ s}^{-1}$	Kugel and Goodrich (2000), Narayan et al. (1994) and Zhu and Winans (1999)
k_{-4}	Transcription of I, binding of D, “off” rate	$4.0 \times 10^{-2} \text{ s}^{-1}$	Kugel and Goodrich (2000), Narayan et al. (1994) and Zhu and Winans (1999)
k_5	Degradation of I mRNA	$6.0 \times 10^{-3} \text{ s}^{-1}$	Hambraeus et al. (2003)
k_6	Translation of R mRNA	$1.6 \times 10^{-2} \text{ s}^{-1}$	Kierzek et al. (2001), Iyer and Struhl (1996) and Watson et al. (2003)
k_7	Degradation of R	10^{-4} s^{-1}	Pratt et al. (2002)
k_8	Binding between R and A	$10^{-5} \text{ m}^{-1} \text{ s}^{-1}$	Estimated
k_{-8}	Dissociation of P	$3.33 \times 10^{-3} \text{ s}^{-1}$	Estimated
k_9	Translation of I mRNA	$1.6 \times 10^{-2} \text{ s}^{-1}$	Kierzek et al. (2001), Iyer and Struhl (1996) and Watson et al. (2003)
k_{10}	Degradation of I	10^{-4} s^{-1}	Pratt et al. (2002)
k_{11}	Enzymatic production of A	$6.0 \times 10^{-2} \text{ s}^{-1}$	Parsek et al. (1999) and Schaefer et al. (1996)
k_{12}	Constitutive transcription of I	$4.0 \times 10^{-4} \text{ m s}^{-1}$	Dundr et al. (2002), Kierzek et al. (2001) and Iyer and Struhl (1996)
k_{13}	Dimerization of P	$10^{-5} \text{ m}^{-1} \text{ s}^{-1}$	Estimated
k_{-13}	Dissociation of D	10^{-2} s^{-1}	Estimated
k_{14}	Autoinducer diffusivity	0.23 s^{-1}	Kaplan and Greenberg (1985) and Rubinow (2002)

All values are adjusted to concentrations expressed as molecules per cell (abbreviated as m). Derived constants are $K_4 = k_{-4}/k_4$, $K_8 = k_8/k_{-8}$ and $K_{13} = k_{13}/k_{-13}$.

is indeed the minimal layout that satisfies the basic QS requirement.

We imitated the adaptive evolution of the intracellular QS network by varying its parameters within a biologically realistic range while trying to achieve simultaneous fulfillment of the following requirements:

- The network should experience the transition to the “on” state at a low extracellular concentration of autoinducer in the range corresponding to 5–10 molecules per cell.
- Concentration of D at $A_e = 0$ should not exceed 0.05 molecules per cell.
- The concentration of D should jump during the transition by at least one order of magnitude.

The results of this naïve empirical optimization are reflected in Table 1 and Fig. 2. We observe that to achieve the stated objectives, the stability of complexes P and D indeed has to be fairly low with the dissociation constants 1 and 3 μM , respectively. Generally, the behavior of the network is found to be highly sensitive to the variation of kinetic parameters and the bistability observed in a very narrow parameter region.

Unexpectedly, we find that the stochastic behavior of the full model deviates from the deterministic dynamics of the ODEs. Fig. 2B presents an averaged over very long observation period ($6 \times 10^6 \text{ s}$) concentration

of D versus A_e plotted together with the deterministic bifurcation diagram. It shows that the stochastic system fails to display a sharp switch-like transition and instead exhibits incremental growth of D concentration that lags behind the deterministic prediction. The difference between stochastic and deterministic values of other network variables is on the order of the numeric precision at $A_e = 0$ and slightly increases with A_e up to the point of transition. Detailed analysis of the D time series shows that the associated probability density function (PDF) peaks at 0 and then decays exponentially with D for all A_e values in the shown range. The observed growth in the average D value is achieved solely through the accumulation of the progressively increasing fluctuations. This result indicates that the minimal network layout may not perform adequately in the conditions of molecular noise and therefore does not comply with all of the requirements for the functional QS network.

3.3. The basal QS network

Introduction of the second positive feedback loop puts concentration levels of both R and A under the control of the transcription factor. We first examine the simplest QS network layout that includes both feedback loops, namely when the dimerization of the transcription factor does not occur. Following the same procedure as was used for the reduction of the minimal network, after the

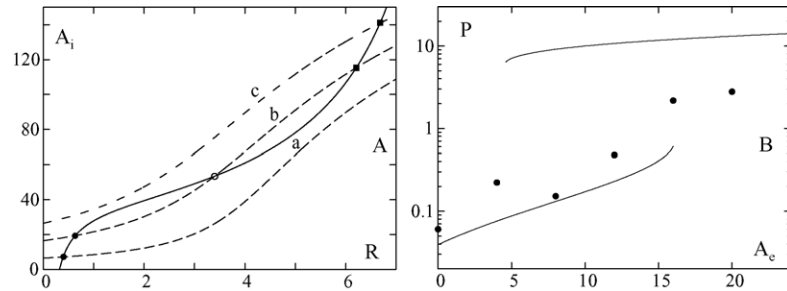


Fig. 3. Behavior of the basal quorum sensing network. (A) The nullclines of the reduced basal model at three values of extracellular autoinducer concentration: (a) 0 nM; (b) 30 nM; (c) 50 nM. R nullcline is shown by solid line. Other notations are the same as in Fig. 2. (B) Dependence of the P concentration on A_e , deterministic bifurcation diagram is shown by lines and time-averaged value of P in the stochastic model by filled circles (observation time 6×10^6 s, sampled every 100 s).

necessary algebra, we arrive at the two equations for R and A:

$$\frac{dA_i}{dt} = \frac{k_{11}k_9}{k_5k_{10}} \left(\frac{k_3RA_i}{K_4/K_8 + RA_i} + k_{12} \right) + k_{14}(A_e - A_i), \quad (9)$$

$$\frac{dR}{dt} = \frac{k_6}{k_2} \left(\frac{k_{15}RA_i}{K_{16}/K_8 + RA_i} + k_1 \right) - k_7R. \quad (10)$$

Systems of equations analogues to the systems (9) and (10) first appeared in the work on the QS phenomenon in *V. fischeri* (James et al., 2000) and later in the independent study on the QS network in *Pseudomonas aeruginosa* (Dockery and Keener, 2001). Owing to the apparent ubiquity of this network layout, in following we refer to it

as the basal. Fig. 3A shows the nullclines of the systems (9) and (10) with the parameter values selected to satisfy the QS network requirements. The geometry of the nullclines is such that the levels of both R and A have to be kept low in the “on” state to ensure that the “off” state is the only stationary point at low A_e . We achieve this by assuming weakness of the I promoter, low transcription rate of R and its fast degradation rate (see Table 2). Additional constraint, common to all models considered here, is that the stability of the “off” state defined by the constitutive transcription levels of I and R comes at a price of high value for the critical extracellular autoinducer concentration.

Stochastic simulations of the network dynamics demonstrate that fluctuations in molecular copy number

Table 2
Kinetic constants used in the model of the basal QS network

Constant	Legend	Value	References
k_1	Constitutive transcription of R	$1.5 \times 10^{-4} \text{ m s}^{-1}$	Dundr et al. (2002), Kierzek et al. (2001) and Iyer and Struhl (1996)
k_3	Transcription of I, maximal velocity	$4.16 \times 10^{-3} \text{ m s}^{-1}$	Dundr et al. (2002), Kierzek et al. (2001) and Iyer and Struhl (1996)
k_4	Transcription of I, binding of P, “on” rate	$10^{-3} \text{ m}^{-1} \text{ s}^{-1}$	Kugel and Goodrich (2000), Narayan et al. (1994) and Zhu and Winans (1999)
k_{-4}	Transcription of I, binding of P, “off” rate	$1.32 \times 10^{-2} \text{ s}^{-1}$	Kugel and Goodrich (2000), Narayan et al. (1994) and Zhu and Winans (1999)
k_6	Translation of R mRNA	$1.28 \times 10^{-2} \text{ s}^{-1}$	Kierzek et al. (2001), Iyer and Struhl (1996) and Watson et al. (2003)
k_7	Degradation of R	10^{-3} s^{-1}	Pratt et al. (2002)
k_8	Binding between R and A	$1.4 \times 10^{-4} \text{ m}^{-1} \text{ s}^{-1}$	Estimated
k_{-8}	Dissociation of P	10^{-2} s^{-1}	Estimated
k_{11}	Enzymatic production of A	$3.3 \times 10^{-1} \text{ s}^{-1}$	Parsek et al. (1999) and Schaefer et al. (1996)
k_{12}	Constitutive transcription of I	$1.17 \times 10^{-4} \text{ m s}^{-1}$	Dundr et al. (2002), Kierzek et al. (2001) and Iyer and Struhl (1996)
k_{14}	Autoinducer diffusivity	0.16 s^{-1}	Kaplan and Greenberg (1985) and Rubino (2002)
k_{15}	Transcription of R, maximal velocity	$4.0 \times 10^{-3} \text{ m s}^{-1}$	Dundr et al. (2002), Kierzek et al. (2001) and Iyer and Struhl (1996)
k_{16}	Transcription of R, binding of P, “on” rate	$10^{-2} \text{ m}^{-1} \text{ s}^{-1}$	Kugel and Goodrich (2000), Narayan et al. (1994) and Zhu and Winans (1999)
k_{-16}	Transcription of R, binding of P, “off” rate	$4.5 \times 10^{-2} \text{ s}^{-1}$	Kugel and Goodrich (2000), Narayan et al. (1994) and Zhu and Winans (1999)

Not displayed constants are the same as in Table 1. Derived constants are $K_4 = k_{-4}/k_4$, $K_8 = k_8/k_{-8}$ and $K_{16} = k_{-16}/k_{16}$.

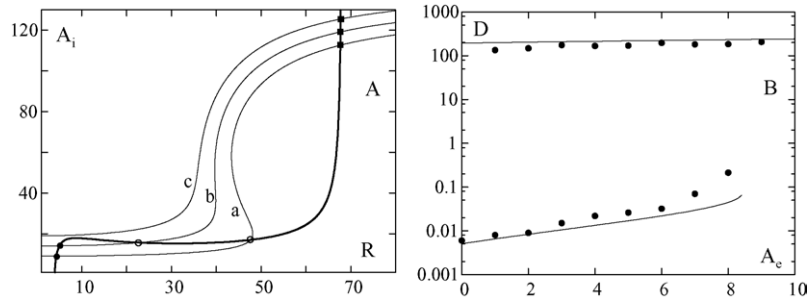


Fig. 4. Dynamics of the modified basal model. (A) The nullclines of the reduced model at three values of A_e : (a) 0 nM; (b) 15 nM; (c) 30 nM. R nullcline is shown in thick solid line. (B) Stationary concentration of D vs. A_e . Stochastic data (filled circles) are plotted together with the deterministic bifurcation diagram.

destroy the bistability of the deterministic model. At the low values of A_e , P exhibits rare but prominent departures from zero. As A_e increases, these excursions quickly grow in amplitude and frequency while the mode of the D PDF remains at 0 for all values of A_e in the shown range. Above the critical autoinducer concentration predicted by the ODEs, it is possible to observe 20–40 copies of P per cell while the average concentration remains much lower than the value that follows from the deterministic model. Thus clear separation between the “off” and “on” states is not preserved in the conditions of molecular noise.

3.4. The basal QS network with dimerization

Finally we modify the basal network layout to include dimerization of the transcription factor. Assuming that the steady-state approximation for concentrations of P and D holds under the earlier specified conditions, the equations for A and R become:

$$\frac{dA_i}{dt} = \frac{k_{11}k_9}{k_5k_{10}} \left(\frac{k_3R^2A_i^2}{K_4/K_{13}K_8^2 + R^2A_i^2} + k_{12} \right) + k_{14}(A_e - A_i), \quad (11)$$

Table 3
Kinetic constants used in the model of the modified basal QS network

Constant	Legend	Value	References
k_1	Constitutive transcription of R	$3.0 \times 10^{-4} \text{ m s}^{-1}$	Dundr et al. (2002), Kierzek et al. (2001) and Iyer and Struhl (1996)
k_3	Transcription of I, maximal velocity	$2.0 \times 10^{-3} \text{ m s}^{-1}$	Dundr et al. (2002), Kierzek et al. (2001) and Iyer and Struhl (1996)
k_4	Transcription of I, binding of D, “on” rate	$10^{-3} \text{ m}^{-1} \text{ s}^{-1}$	Kugel and Goodrich (2000), Narayan et al. (1994) and Zhu and Winans (1999)
k_{-4}	Transcription of I, binding of D, “off” rate	$3.0 \times 10^{-2} \text{ s}^{-1}$	Kugel and Goodrich (2000), Narayan et al. (1994) and Zhu and Winans (1999)
k_7	Degradation of R	$2.0 \times 10^{-4} \text{ s}^{-1}$	Pratt et al. (2002)
k_8	Binding between R and A	$10^{-4} \text{ m}^{-1} \text{ s}^{-1}$	Estimated
k_{-8}	Dissociation of P	$3.0 \times 10^{-3} \text{ s}^{-1}$	Estimated
k_{10}	Degradation of I	$5.0 \times 10^{-5} \text{ s}^{-1}$	Pratt et al. (2002)
k_{11}	Enzymatic production of A	0.45 s^{-1}	Parsek et al. (1999) and Schaefer et al. (1996)
k_{12}	Constitutive transcription of I	$1.5 \times 10^{-4} \text{ m s}^{-1}$	Dundr et al. (2002), Kierzek et al. (2001) and Iyer and Struhl (1996)
k_{13}	Dimerization of P	$3.0 \times 10^{-5} \text{ m}^{-1} \text{ s}^{-1}$	Estimated
k_{14}	Autoinducer diffusivity	0.4 s^{-1}	Kaplan and Greenberg (1985) and Rubinow (2002)
k_{15}	Transcription of R, maximal velocity	$4.8 \times 10^{-3} \text{ m s}^{-1}$	Dundr et al. (2002), Kierzek et al. (2001) and Iyer and Struhl (1996)
k_{16}	Transcription of R, binding of D, “on” rate	$10^{-2} \text{ m}^{-1} \text{ s}^{-1}$	Kugel and Goodrich (2000), Narayan et al. (1994) and Zhu and Winans (1999)
k_{-16}	Transcription of R, binding of D, “off” rate	10^{-2} s^{-1}	Kugel and Goodrich (2000), Narayan et al. (1994) and Zhu and Winans (1999)

Not shown constants are the same as in Table 1. Derived constants are $K_4 = k_{-4}/k_4$, $K_8 = k_8/k_{-8}$, $K_{13} = k_{13}/k_{-13}$ and $K_{16} = k_{-16}/k_{16}$.

$$\frac{dR}{dt} = \frac{k_6}{k_2} \left(\frac{k_{15} R^2 A_1^2}{K_{16}/K_{13} K_8^2 + R^2 A_1^2} + k_1 \right) - k_7 R. \quad (12)$$

The increase in the nonlinearity of the system is accompanied by the drastic change in the shape of the nullclines presented in Fig. 4A. Demanding that the network should not possess the “on” state at $A_e = 0$ would require further reduction in the strength of both R and I promoters. Instead here we consider the case when the network is formally bistable already in the absence of extracellular autoinducer. To reduce the risk of spontaneous transition to the “on” state in the conditions of molecular noise, we optimize the network parameters (see Table 3) for stability of the “off” state at $A_e = 0$. The resulting model demonstrates bistable behavior also in the stochastic simulations (see Fig. 4B). Introduction of the dimerization step effectively abolishes large sporadic excursions away from the “off” state typical to the basal model. In accordance with the prediction of the deterministic system, the “off” state ceases to exist beyond the critical value of A_e . Interestingly, we find a significant difference in the relative stability of the “off” and “on” states depending on the value of A_e . At $A_e = 0$, a simulation trajectory started in the “off” state remains their indefinitely long (at least for $\geq 10^7$ s or 115 days used as an upper limit in our simulations). On the contrary, a simulation with initial conditions corresponding to the “on” state very quickly reaches the “off” state. As A_e grows, the relative stability changes in favor of the “on” state. Thus for $A_e \geq 5$, the system spontaneously escapes into the “on” state during our standard observation time of 6 million seconds. This behavior, while formally undesirable, may not present a biologically significant problem since the concentration range of extracellular autoinducer where it occurs would normally be reached only during the transition to QS. More importantly for the biological function, the network appears to be stable in the “off” state in the neighborhood of $A_e = 0$.

4. Conclusions

Here we considered the behavior of several structural variations of a prototypical QS network differing in the presence of additional amplification loop and the dimerization of the transcription factor. For each layout we attempted to identify a set of parameters that optimizes the functional fitness of the network. The search in the parameter space is constrained by requesting that the kinetic parameters must remain in the biologically realistic range and the resulting network should demonstrate the behavior compatible with our present under-

standing of the quorum sensing phenomenon. Although our analysis is not exhaustive, it helps to understand the importance of certain common components of the control circuitry. Thus, dimerization of the transcription factor is found to be important both with and without the additional feedback loop. Dimerization reduces the noise of the “off” state and improves its stability. Both dimerization and the R self-amplification loop are necessary to provide significant difference (two to three orders of magnitude) between the levels of the transcription factor in the “off” and “on” states. This separation appears to be necessary for preservation of the switch-like behavior when fluctuations in the molecular copy numbers are included into the consideration.

All discussed network layouts consist solely of positive feedback loops. The very existence of the “off” state in such systems depends on the weakness of binding between autoinducer and the monomeric transcription factor as well as between the monomers if dimerization is involved. If these conditions on the kinetic constants are not observed, the quorum sensing effect cannot be achieved with the layout considered here. Secondly, for the stability of the “off” state it is important that the expression of both R and I is only weakly induced by the transcription factor. This implies that the network requires a long period of time to switch into the “on” state, since this transition is based on the accumulation of R and I. Furthermore, the stabilization of the “off” state comes together with an inevitable increase in the critical concentration of autoinducer. Taken together, these observations highlight that a network design based solely on positive feedback is not efficient for construction of “on–off” gene expression switches. We therefore predict that the future research in quorum sensing will emphasize the importance of additional negative feedback loops, like the one found in the QS network of *A. tumefaciens*.

Acknowledgements

We thank Lian Hui Zhang for many fruitful discussions of bacterial quorum sensing. This work was supported by the Agency for Science, Technology and Research, Singapore.

References

- Basu, S., Mehreja, R., Thiberge, S., Chen, M.T., Weiss, R., 2004. Spatiotemporal control of gene expression with pulse-generating networks. *Proc. Natl. Acad. Sci. U.S.A.* 101, 6355–6360.
- Dhar, P., Meng, T.C., Somani, S., Ye, L., Sairam, A., Chitre, M., Hao, Z., Sakharkar, K., 2004a. Cellware—a multi-algorithmic software for computational systems biology. *Bioinformatics* 20, 1319–1321.

- Dhar, P., Meng, T.C., Somani, S., Ye, L., Sakharkar, K., Krishnan, A., Ridwan, A.B., Chitre, M., Hao, Z., 2004b. Grid Cellware: the first grid-enabled tool for modeling and simulating cellular processes. *Bioinformatics*.
- Dockery, J.D., Keener, J.P., 2001. A mathematical model for quorum sensing in *Pseudomonas aeruginosa*. *Bull. Math. Biol.* 63, 95–116.
- Dundr, M., Hoffmann-Rohrer, U., Hu, Q., Grummt, I., Rothblum, L.I., Phair, R.D., Misteli, T., 2002. A kinetic framework for a mammalian RNA polymerase in vivo. *Science* 298, 1623–1626.
- Engelbrecht, J., Neelson, K., Silverman, M., 1983. Bacterial bioluminescence: isolation and genetic analysis of functions from *Vibrio fischeri*. *Cell* 32, 773–781.
- Engelbrecht, J., Silverman, M., 1984. Identification of genes and gene products necessary for bacterial bioluminescence. *Proc. Natl. Acad. Sci. U.S.A.* 81, 4154–4158.
- Fuqua, C., Greenberg, E.P., 2002. Listening in on bacteria: acyl-homoserine lactone signalling. *Nat. Rev. Mol. Cell Biol.* 3, 685–695.
- Fuqua, C., Parsek, M.R., Greenberg, E.P., 2001. Regulation of gene expression by cell-to-cell communication: acyl-homoserine lactone quorum sensing. *Annu. Rev. Genet.* 35, 439–468.
- Gillespie, D.T., 1977. Exact stochastic simulation of coupled chemical reactions. *J. Phys. Chem.* 81, 2340–2361.
- Hambraeus, G., von Wachenfeldt, C., Hederstedt, L., 2003. Genome-wide survey of mRNA half-lives in *Bacillus subtilis* identifies extremely stable mRNAs. *Mol. Genet. Genomics* 269, 706–714.
- Hartwell, L.H., Hopfield, J.J., Leibler, S., Murray, A.W., 1999. From molecular to modular cell biology. *Nature* 402, C47–C52.
- Henke, J.M., Bassler, B.L., 2004. Bacterial social engagements. *Trends Cell Biol.* 14, 648–656.
- Hwang, I., Smyth, A.J., Luo, Z.Q., Farrand, S.K., 1999. Modulating quorum sensing by antiactivation: TraM interacts with TraR to inhibit activation of Ti plasmid conjugal transfer genes. *Mol. Microbiol.* 34, 282–294.
- Ideker, T., Galitski, T., Hood, L., 2001. A new approach to decoding life: systems biology. *Annu. Rev. Genomics Hum. Genet.* 2, 343–372.
- Iyer, V., Struhl, K., 1996. Absolute mRNA levels and transcriptional initiation rates in *Saccharomyces cerevisiae*. *Proc. Natl. Acad. Sci. U.S.A.* 93, 5208–5212.
- James, S., Nilsson, P., James, G., Kjelleberg, S., Fagerstrom, T., 2000. Luminescence control in the marine bacterium *Vibrio fischeri*: an analysis of the dynamics of lux regulation. *J. Mol. Biol.* 296, 1127–1137.
- Kaplan, H.B., Greenberg, E.P., 1985. Diffusion of autoinducer is involved in regulation of the *Vibrio fischeri* luminescence system. *J. Bacteriol.* 163, 1210–1214.
- Kierzek, A.M., Zaim, J., Zielenkiewicz, P., 2001. The effect of transcription and translation initiation frequencies on the stochastic fluctuations in prokaryotic gene expression. *J. Biol. Chem.* 276, 8165–8172.
- Kugel, J.F., Goodrich, J.A., 2000. A kinetic model for the early steps of RNA synthesis by human RNA polymerase II. *J. Biol. Chem.* 275, 40483–40491.
- Ledgham, F., Ventre, I., Soscia, C., Foglino, M., Sturgis, J.N., Lazdunski, A., 2003. Interactions of the quorum sensing regulator QscR: interaction with itself and the other regulators of *Pseudomonas aeruginosa* LasR and RhIR. *Mol. Microbiol.* 48, 199–210.
- McMillen, D., Kopell, N., Hasty, J., Collins, J.J., 2002. Synchronizing genetic relaxation oscillators by intercell signaling. *Proc. Natl. Acad. Sci. U.S.A.* 99, 679–684.
- Milo, R., Shen-Orr, S., Itzkovitz, S., Kashtan, N., Chklovskii, D., Alon, U., 2002. Network motifs: simple building blocks of complex networks. *Science* 298, 824–827.
- Narayan, S., Widen, S.G., Beard, W.A., Wilson, S.H., 1994. RNA polymerase II transcription. Rate of promoter clearance is enhanced by a purified activating transcription factor/cAMP response element-binding protein. *J. Biol. Chem.* 269, 12755–12763.
- Parsek, M.R., Val, D.L., Hanzelka, B.L., Cronan Jr., J.E., Greenberg, E.P., 1999. Acyl homoserine-lactone quorum-sensing signal generation. *Proc. Natl. Acad. Sci. U.S.A.* 96, 4360–4365.
- Pratt, J.M., Petty, J., Riba-Garcia, I., Robertson, D.H., Gaskell, S.J., Oliver, S.G., Beynon, R.J., 2002. Dynamics of protein turnover, a missing dimension in proteomics. *Mol. Cell Proteomics* 1, 579–591.
- Rubinow, S.I., 2002. *Introduction to Mathematical Biology*. Dover Publications, New York.
- Schaefer, A.L., Val, D.L., Hanzelka, B.L., Cronan Jr., J.E., Greenberg, E.P., 1996. Generation of cell-to-cell signals in quorum sensing: acyl homoserine lactone synthase activity of a purified *Vibrio fischeri* LuxI protein. *Proc. Natl. Acad. Sci. U.S.A.* 93, 9505–9509.
- Swiderska, A., Berndtson, A.K., Cha, M.R., Li, L., Beaudoin III, G.M., Zhu, J., Fuqua, C., 2001. Inhibition of the *Agrobacterium tumefaciens* TraR quorum-sensing regulator. Interactions with the TraM anti-activator. *J. Biol. Chem.* 276, 49449–49458.
- Urbanowski, A.L., Lostroh, C.P., Greenberg, E.P., 2004. Reversible acyl-homoserine lactone binding to purified *Vibrio fischeri* LuxR protein. *J. Bacteriol.* 186, 631–637.
- von Bodman, S.B., Bauer, W.D., Coplin, D.L., 2003. Quorum sensing in plant-pathogenic bacteria. *Annu. Rev. Phytopathol.* 41, 455–482.
- Watson, J.D., Hopkins, N.H., Roberts, J.W., Steitz, J.A., Weiner, A.M., 2003. *Molecular Biology of the Gene*. Benjamin Cummings, New York.
- Wisniewski-Dye, F., Downie, J.A., 2002. Quorum-sensing in *Rhizobium*. *Antonie Van Leeuwenhoek Int. J. Gen. Mol. Microbiol.* 81, 397–407.
- You, L.C., Cox, R.S., Weiss, R., Arnold, F.H., 2004. Programmed population control by cell–cell communication and regulated killing. *Nature* 428, 868–871.
- Zhang, R.G., Pappas, T., Brace, J.L., Miller, P.C., Oulmassov, T., Molyneaux, J.M., Anderson, J.C., Bashkin, J.K., Winans, S.C., Joachimiak, A., 2002. Structure of a bacterial quorum-sensing transcription factor complexed with pheromone and DNA. *Nature* 417, 971–974.
- Zhu, J., Oger, P.M., Schrammeijer, B., Hooykaas, P.J., Farrand, S.K., Winans, S.C., 2000. The bases of crown gall tumorigenesis. *J. Bacteriol.* 182, 3885–3895.
- Zhu, J., Winans, S.C., 1999. Autoinducer binding by the quorum-sensing regulator TraR increases affinity for target promoters in vitro and decreases TraR turnover rates in whole cells. *Proc. Natl. Acad. Sci. U.S.A.* 96, 4832–4837.
- Zhu, J., Winans, S.C., 2001. The quorum-sensing transcriptional regulator TraR requires its cognate signaling ligand for protein folding, protease resistance, and dimerization. *Proc. Natl. Acad. Sci. U.S.A.* 98, 1507–1512.